

---

# A RE-CALIBRATION METHOD FOR OBJECT DETECTION WITH MULTI-MODAL ALIGNMENT BIAS IN AUTONOMOUS DRIVING

---

Zhihang Song, Lihui Peng\*, Jianming Hu, Danya Yao, Yi Zhang

Department of Automation

Tsinghua University

Beijing, China

song-zh22@mails.tsinghua.edu.cn, lihuipeng@mail.tsinghua.edu.cn

## ABSTRACT

Multi-modal object detection in autonomous driving has achieved great breakthroughs due to the usage of fusing complementary information from different sensors. The calibration in fusion between sensors such as LiDAR and camera is always supposed to be precise in previous work. However, in reality, calibration matrices are fixed when the vehicles leave the factory, but vibration, bumps, and data lags may cause calibration bias. As the research on the calibration influence on fusion detection performance is relatively few, flexible calibration dependency multi-sensor detection method has always been attractive. In this paper, we conducted experiments on SOTA detection method EPNet++ and proved slight bias on calibration can reduce the performance seriously. We also proposed a re-calibration model based on semantic segmentation which can be combined with a detection algorithm to improve the performance and robustness of multi-modal calibration bias.

**Keywords** Calibration, Multi-modal, Object Detection

## 1 Introduction

The object detection is a major element in the environment perception of autonomous driving. Many brilliant works have been made based on different sensor inputs such as camera[1],[2], LiDAR[3],[4],[5], or both of them[6],[7],[8],[9]. Nowadays, the multi-modal fusion method has become a trend for 3D detection tasks. Due to the usage of complementary data from different sensors, such as image and point cloud, the multi-modal fusion method can achieve better performance than single-sensor ones. However, besides the advantages, multi-modal fusion also brings new challenges for algorithms. As the data representation from different sensors can be quite different, a unique model structure design is a must to integrate features from each modal. Also, sensors in different locations have to be calibrated to share the same world coordinate so that the information can be correctly aligned and fused. Previous works have made lots of breakthroughs for the first challenge by using sequential fusion[10], bird's eye fusion[9],[11], LiDAR-guided image fusion[12], etc.

However, for the sensor calibration problem, the calibration matrices are always taken as fixed and perfectly given in the 3D object detection process. Training for 3D object detection often uses well-processed datasets such as KITTI dataset[13], giving precise calibration matrices per frame. Some data collection vehicles such as in ONCE dataset[14] are corrected daily for calibration, which is not the situation in real driving. Previous studies in calibration mainly focus on the calibration process before vehicles get out of the factory and the calibration is then fixed and doesn't need to be considered in perception tasks. However, in reality, vehicles on roads may encounter bumps and vibrations[15]. Because the LiDAR scans its surroundings in a period but the camera takes images instantaneously, it might cause bias in calibration information too. There may also exist data delays and sensor drifts which can also influence the calibration performance[15].

Recently, some researchers have also paid attention to the calibration influence on 3D object detection performance. Two benchmarking works[16], [15] in 2023 indicated that alignment bias like other data corruptions such as weather

---

\* Corresponding author: Lihui Peng.

and motion compensation, are challenging to fusion models. Since multi-modal fusion detection heavily depends on the feature alignment, the accuracy of calibration is of great importance. Yet, most calibration studies are designed for offline experiments with defined targets to provide the user with one-time precise calibration parameters, which need hours and specific experimental fields. Some recent targetless deep-learning-based calibration algorithms use iterative methods[17] or Brute-force search[18] to complete the calibration correctness, but these methods also take several seconds or minutes to finish and can't be used in detection tasks. As the studies for calibration correctness in 3D object detection are relatively few, we developed a flexible and fast re-calibration detection framework to deal with the calibration bias and noises.

Our work uses semantic segmentation features to guide the re-calibration inference and design a unique loss and training process. The re-calibration module takes the image, point cloud, and initial rough calibration as inputs and outputs corrected calibration before sending them into the 3D object detection module. In our experiments, we implemented the EPNet++[19] as the detection test model, which has an advanced performance in multi-modal algorithms. We conducted two types of calibration corruption experiments. One is the calibration matrices have random noise or bias, and the other is the LiDAR point cloud location in world coordinates has a small translation. We conducted a series of experiments and demonstrated that our method can significantly improve the performance of 3D detection method in both corruptions. The latest related work GraphAlign++[20] achieves great robustness in calibration Gaussian noise by designing the perception algorithm structure. Our work came up with a modular re-calibration framework in another aspect, so it can be easily shifted to different detection methods as well as other calibration-dependant tasks without modifying perception models.

The main contributions of this work include: (a) Experiments in our study support the view that spatial misalignment has great impact on 3D detection tasks. (b) We proposed a simple but effective framework to re-calibrate the misalignment in detection tasks. (c) We designed a fast and flexible re-calibration model and training method for the framework.

This paper begins with Section 2 to introduce relative works in the field of calibration and 3D detection. In Sections 3, we describe our re-calibration detection framework from data preparation, structure design, and loss design in detail, respectively. In Section 4, we conducted experiments on the baseline and our re-calibration model, which proves the influence of calibration bias in detection work and shows our improved results. Finally, we discuss some perspectives for future research and provide a summary in Section 5.

## 2 Related Works

### 2.1 LiDAR-Camera 3D Object Detection

There are many studies in 3D object detection, and we only focus on those with multi-modal inputs of LiDAR and camera. As the LiDAR point clouds can provide depth and location information while cameras have an advantage in capturing texture and detail information, it's of great means to utilize both complementary features to improve the detection performance. Related works can be categorized mainly into three fusion types, i.e. point-level, feature-level, and proposal-level fusion.

The point-level fusion method fuses the feature information obtained from the camera into the LiDAR point cloud, and enhances the expression ability of points by projection. Early typical methods contain PointPainting[7], FusionPainting[21], etc. These methods extract semantic information from the camera to augment each point and then use the point cloud detection head to complete the task. Other approaches such as EPNet[12], EPNet++[19], PointAugmenting[8], and FocalsConv[22] implement richer features and more refined fusion methods to achieve better detection results. The feature-level fusion method extracts features from two input modalities and fuses them into one feature space by designed networks. Many outstanding studies implement Transformer-based structures to align features into LiDAR coordinates[23, 24, 25, 26] or bird's eye view space[9, 11, 20, 27]. The proposal-level fusion method typically involves two independent extractors to generate 3D bounding box predictions for both modalities and then use post-processing techniques to fuse these decisions[28, 29, 30].

### 2.2 LiDAR-Camera Calibration

The calibration of extrinsic parameters is to determine the relationship between the positions and directions of different sensors. The extrinsic calibration matrix can be used to project different sensor data into a unified coordinate system, thereby completing the fusion of multi-modal information[31]. Existing extrinsic calibration methods for LiDAR and camera can be broadly categorized into target-based and target-free types, and the target-free type can be further divided into feature-based and learning-based methods[32].

The target-based methods depend on rigs, which are specific objects mostly with regular shapes and distinctive patterns[33, 34, 35, 36]. The optimization algorithm is then applied to align easily extracted geometric features. The feature-based target-free methods use geometric features detected from the real world to complete the alignments[37]. Commonly used geometric features are edges and lines in scenes[38]. When detected, features like lines are aligned to their correspondence with location information and then used to calculate the calibration[38, 39]. Besides geometric features, more indirect features such as vanishing points[40, 41], intensity, and color channels[31, 42] are also used to estimate calibration.

With the stunning development of deep learning, learning-based extrinsic calibration methods also emerged to solve the calibration problem. By using perception methods to extract features, end-to-end networks are developed to estimate calibration parameters from raw sensor inputs[43, 44, 45]. The odometry information is adopted in spatial and temporal parameter estimation[46, 47]. In 2021, LCCNet is developed to predict the extrinsic parameters in real-time[48]. [49] proposed a calibration method based on Gaussian processes estimated moving target trajectories. Such methods are limited by the odometry and tracking results[18]. Besides, semantic segmentation features are also widely adopted for calibrating LiDAR and cameras[17, 50, 51]. Calib-Anything utilizes the large model SAM[52] to deal with the input data and uses the Brute-force searching method for calibration[18]. Some methods such as SST-Calib also used combined features of visual odometry and semantic segmentation to infer spatial-temporal parameters[32]. In 2024, CalibFormer implemented a transformer-based correlation head to align features for calibration[53]. The Target-free methods based on deep learning broaden the usage limits of the situation and thus attract more and more attention.

### 3 Methodology

In this section, we will introduce our re-calibration object detection framework in detail. The framework contains two parts, one is the re-calibration module, and the other is the calibration dependant LiDAR-camera fusion detection module, which can be replaced with any algorithm needed. When there exists bias in calibration matrices or translation in the point cloud, we first send the sensor outputs and calibration parameters into the instant re-calibration module to inference the proper calibration between the LiDAR and the camera. Then, the re-calibration parameters are fed to the detection module to complete perception tasks.

We first show how we prepare the data and proper labels for training; we then introduce the model structure design for our semantic-segmentation re-calibration module. Finally, we describe our loss design and tricks in the training process.

#### 3.1 Data Preparation

In order to train the re-calibration module, we first need to establish training datasets with calibration bias inputs and precise labels. We chose KITTI dataset[13] as our data source and designed two types of alignment bias to augment our training set, i.e. random noise and point cloud translation.

**Random Noise:** The first type is random noise in calibration matrices. This kind of noise can represent the bias in calibration initialization and the latter changes in driving bumps and vibration. We made this kind of data by adding Gaussian noises with different variances to the extrinsic matrix. However, this kind of noise is not enough for re-calibration training because all the calibration labels in KITTI are close to several specific matrices which may lead to a short-cut learning of regression to fixed values. Also, the Gaussian noise can not represent to point cloud location bias caused by the stuck or drifting sensor. Thus, we also add the point cloud translation as the second data generation method.

**Point Cloud Translation:** To generate different calibration labels with corresponding data, we chose to translate both point cloud data and the extrinsic parameters. As for the point cloud translation, we use the translation matrices and their reverse matrices to generate new point clouds and corresponding labels. The generation is shown as equations below:

$$\underbrace{\begin{bmatrix} x' \\ y' \\ z' \\ 1 \end{bmatrix}^T}_{\text{New point cloud}} = \underbrace{\begin{bmatrix} x \\ y \\ z \\ 1 \end{bmatrix}^T}_{Tr} * \underbrace{\begin{bmatrix} 1 & 0 & 0 & 0 \\ 0 & 1 & 0 & 0 \\ 0 & 0 & 1 & 0 \\ a & b & c & 1 \end{bmatrix}}_{Tr} * \underbrace{Tr^{-1} * V2C^T}_{\text{New extrinsic label}} * R0^T \quad (1)$$

$a, b, c$  are random translation parameters,  $V2C$  and  $R0$  are the extrinsic and rectified matrix. As EPNet++ is based on the point cloud, we also need to translate the object labels simultaneously when combined in the detection evaluation process.

In the whole training process, we use a random variable  $\alpha$  to control which kind of bias is generated or combining both. In this way, we generated different calibration data and labels for training our re-calibration module.

### 3.2 Re-calibration Model structure

For the re-calibration model, we design the algorithm based on semantic-segmentation methods. The whole structure of the re-calibration model is shown in Figure1.

In the first stage, the point cloud and image are sent into two pre-trained semantic segmentation model separately. In our experiments, we chose Cylinder3D[54, 55, 56] for point cloud segmentation and Deeplabv3[57] for image segmentation, which can be replaced by any needed segmentation methods. They are not involved in gradient calculation and parameter update. These segmentation models then output the interested segmentation labels which are determined by the detection tasks. In our experiments, we separate the segmentation of cars as inputs for next stage.

In the second stage, the point cloud segmentation results are projected to the camera pixel coordinates by the input calibration matrices with bias. The projected point segmentation result is then concatenated with image segmentation to generate the alignment feature. The alignment feature contains segmentation information from points and images in the same pixel coordinate system. Thus the clusters of projected points may have displacements with corresponding image areas, which can guide the network to learn the bias of the projection.

Besides, we also want the model to learn the relationship between the input projection matrix parameters and the coordinates bias. Thus, at the same time, we also record the corresponding coordinates in 3D LiDAR coordinate system and 2D camera pixel coordinate system. Then, we select the interested points with the above corresponding coordinates to generate the calibration feature. The calibration feature is arranged in the pixel plane with five position values.  $x, y, z$  are the original positions of LiDAR points, and  $u, v$  are projected pixel positions. In this way, we involved the input projection matrix information in the learning process. The alignment feature and calibration feature is then fed into the fusion net which outputs the extrinsic matrix bias.

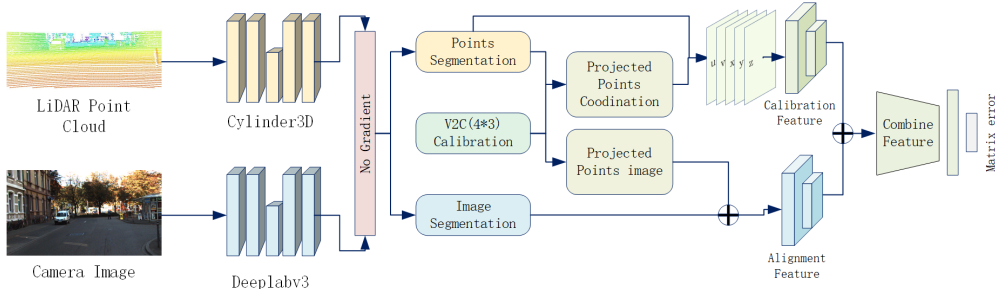


Figure 1: Structure of re-calibration model.

### 3.3 Loss Design

In re-calibration model training, we utilize a composite loss function with two parts. The first one is projected distance loss inspired by semantic alignment loss in SemAlign[17], which uses segmentation information to evaluate the quality of calibration projection. The semantic alignment loss is designed to calculate the distance between the projected point cloud and the same feature in the corresponding image. As our method is supervised and generates variance data with calibration label in 3.1, we can simplify this loss to calculate the distance between output and label projected point clusters. See Figure2. White points are the correct projected position by label calibration. Green points are projected position by output re-calibration results. Projected loss calculates the distance between the points in clusters with the same interested class label. For each re-calibration projected point of a specific class, we calculate its distance to the nearest neighbor in the label projected points clusters. Then we use the sum value of distance as the projected loss. This kind of loss contributes to the model training in learning which elements in the matrix to modify and how they affect projection. Projected loss can be written in 2.  $p_c^i$  refers to the  $i_{th}$  point in projected point cluster of re-calibration and  $p_l^j$  refers to the  $j_{th}$  point in label projected point cluster.  $dist()$  calculates the L2 norm of displacement between two position vectors.

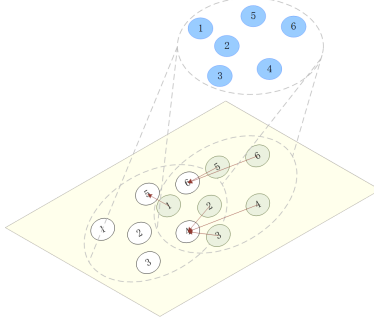


Figure 2: Projected loss.

$$Projected\_loss = \sum_i \min_j (dist(p_c^i, p_l^j)) \quad (2)$$

The other part of our loss function is a normal MSE loss between inference bias and label bias to each element in the extrinsic matrix. This part directly leads the model to learn where to optimize. As the projection from LiDAR world coordinate system to 2D pixel coordinate system is a dimensionality reduction process, there exists infinity solution the the projection alignment matrix. Thus, it's necessary to modify the weights of two loss because the projected loss may lead to another local optimum with similar 2D projection but totally different calibration in 3D. The whole loss design can be expressed as below<sup>3</sup>. In experiment, we set  $\lambda_1$  and  $\lambda_2$  to be 10 and 0.001 to make the model quickly converge. Then, we modify the  $\lambda_1$  and  $\lambda_2$  to be 10 and 0.00001 to let the model converge to the calibration bias we need.

$$Total\_loss = \lambda_1 * MSE(calib_{out} + calib_{in}, calib_{label}) + \lambda_2 * \sum_i \min_j (dist(p_c^i, p_l^j)) \quad (3)$$

## 4 Experiment Results

To verify the re-calibration effects on multi-modal object detection methods, we conduct experiments with the EPNet++ algorithm. Firstly, we test the EPNet++ on the car category in KITTI dataset. By testing the same model with clean calibration, random Gaussian noise and point cloud translation, we proved that little bias in calibration may cause a severe performance drop for the multi-modal detection method using calibration matrices as direct inputs. The results are shown by giving a comparison in Table1. With the Gaussian noise of  $\sigma = 0.01$  added to calibration matrices, all the four AP performance are corrupted. That's because the detection algorithm can't align the features from images and LiDAR points. See Figure3,4, we extracted the fusion feature from RPN net in EPNet++, which shows the impact of calibration bias on the perception algorithm. With added noise, the features of vehicles got blurred or even vanished. The translation in LiDAR points also causes displacement and blur in the fusion feature. Thus, we infer that the severe misaligned fusion feature can't be identified by the fusion detection and causes low recall and AP.

Table 1: Comparison of EPNet++ performance with different calibration bias (Easy)

<i>Data Type</i>	<i>AP@0.7 bbox</i>	<i>AP@0.7 bev</i>	<i>AP@0.7 3d</i>	<i>AP@0.7 aos</i>
KITTI original data+calibration	99.21	96.13	92.79	99.05
KITTI original data+Gaussian noise calibration	58.36	52.03	18.08	58.28
KITTI LiDAR $\delta y=0.2m$ +translated calibration	99.22	96.13	92.78	99.05
KITTI LiDAR $\delta y=0.2m$ +original calibration	95.37	72.18	42.75	95.19

Then we applied our re-calibration module combined with the detection process and tested the performance again. The re-calibration result is shown in Table3, Table4. From the table we can see that the AP of four metrics got significant improvement in the Gaussian noise situation. The AP of 3D and BEV are improved in LiDAR translation situation. After the re-calibration process, although the detection method still can't recover to the ideal level, the performances are more acceptable for serious corruption. We can also see the re-calibration effect from the LiDAR point projected to image coordinates, see Figure5 and Figure6. It's obvious that the points we are interested in have less distance to the label, which makes the feature align from the image and point cloud better.

Table 2: Comparison of EPNet++ performance with different calibration bias (Moderate)

<i>Data Type</i>	<i>AP@0.7 bbox</i>	<i>AP@0.7 bev</i>	<i>AP@0.7 3d</i>	<i>AP@0.7 aos</i>
KITTI original data+calibration	94.19	89.00	83.24	93.17
KITTI original data+Gaussian noise calibration	47.30	42.02	15.19	47.15
KITTI LiDAR $\delta y=0.2m$ +translated calibration	94.19	89.00	83.24	93.17
KITTI LiDAR $\delta y=0.2m$ +original calibration	89.05	66.68	39.20	88.56

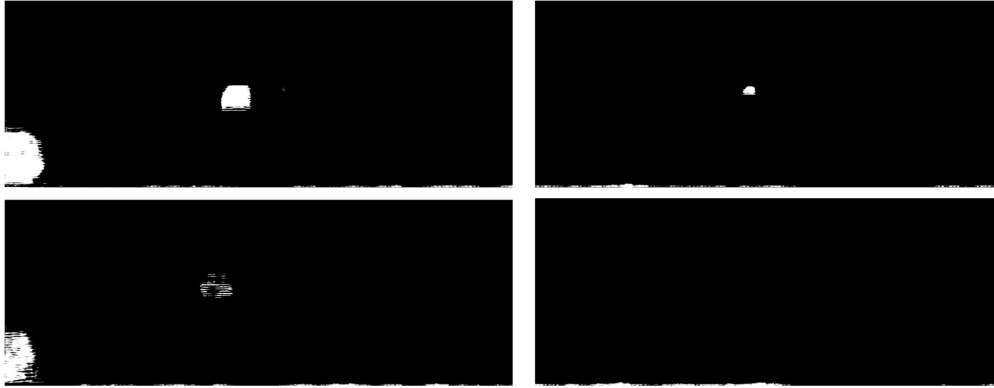


Figure 3: Corrupted feature fusion caused by Gaussian noise in calibration.(Up: without noise. Down: with noise.)

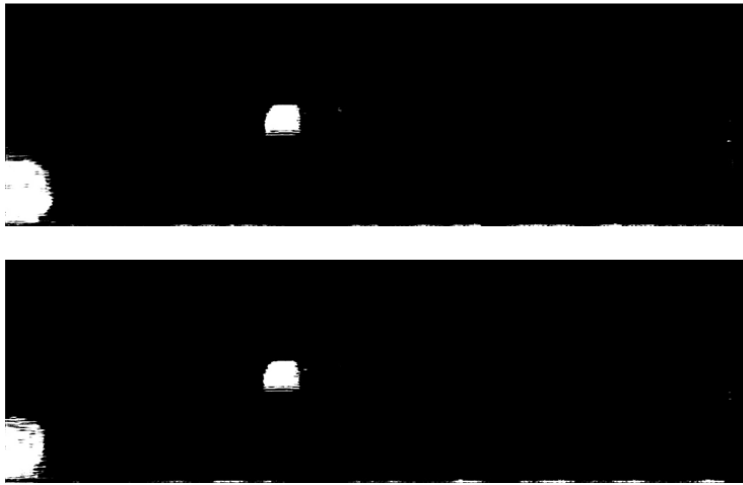


Figure 4: Corrupted feature fusion caused by point translation in LiDAR.(Up: without translation. Down: with translation.)



Figure 5: Comparison of points projection with Gaussian noise in calibration before and after re-calibration.(White: label; Green: before; Blue: After.)



Figure 6: Comparison of points projection with point translation in LiDAR before and after re-calibration.(White: label; Green: before; Blue: After.)

In our experiment, we also found that the improvements in moderate objects and hard objects are not significant enough in comparison to those in easy ones. We analyzed that it might be because the semantic segmentation results are less accurate in the re-calibration model, which influences the feature extraction and alignment to calculate the calibration bias. Thus, one way to further improve the performance of re-calibration detection is to change a better pre-trained image segmentation algorithm and point cloud segmentation algorithm to produce precise segmentation information for calibration.

We also tested the speed of our re-calibration model. Except for the segmentation part without training, the main part of the re-calibration net takes about 40 ms on the NVIDIA RTX3090Ti GPU. The whole time of re-calibration work can be modified by changing the segmentation part and with the Deeplabv3 and Cylinder3D we used, it takes about 0.2-0.4 seconds per frame. Compared to 15-30 seconds consumed by segmentation methods such as SemAlign[17] and CalibAnything[18], our work has great speed advantages.

Table 3: Comparison of EPNet++ performance with re-calibration (Easy)

<i>Data Type</i>	<i>AP@0.7 bbox</i>	<i>AP@0.7 bev</i>	<i>AP@0.7 3d</i>	<i>AP@0.7 aos</i>
KITTI original data+Gaussian noise calibration	58.36	52.03	18.08	58.28
KITTI original data+Gaussian noise re-calibration	83.48	57.67	35.38	83.37
KITTI LiDAR $\delta y=0.2m$ +original calibration	95.37	72.18	42.75	95.19
KITTI LiDAR $\delta y=0.2m$ +re-calibration	95.30	80.98	59.13	95.18

Table 4: Comparison of EPNet++ performance with re-calibration (Moderate)

<i>Data Type</i>	<i>AP@0.7 bbox</i>	<i>AP@0.7 bev</i>	<i>AP@0.7 3d</i>	<i>AP@0.7 aos</i>
KITTI original data+Gaussian noise calibration	47.30	42.02	15.19	47.15
KITTI original data+Gaussian noise re-calibration	71.61	45.82	27.01	71.37
KITTI LiDAR $\delta y=0.2m$ +original calibration	89.05	66.68	39.20	88.56
KITTI LiDAR $\delta y=0.2m$ +re-calibration	85.44	70.55	46.61	85.05

## 5 Conclusion

This paper provides a flexible re-calibration detection framework to deal with the alignment bias problem in multi-modal perception tasks. Our approach utilizes semantic segmentation information to predict the extrinsic matrix bias and investigates how the calibration bias impacts the detection tasks. We implement our framework to EPNet++ and prove its usability. We hope that our work can provide a new perspective on improving the performance of existing multi-modal detection methods in misalignment bias. The limitation of our work is that the re-calibration model depends on the segmentation results, which faces challenges in complex and hard situations. Our further work will be developed mainly focusing on a better and faster re-calibration model to enhance the performance.

## References

- [1] Jason Ku, Alex D Pon, and Steven L Waslander. Monocular 3d object detection leveraging accurate proposals and shape reconstruction. In *Proceedings of the IEEE/CVF conference on computer vision and pattern recognition*,

- pages 11867–11876, 2019.
- [2] Zongdai Liu, Dingfu Zhou, Feixiang Lu, Jin Fang, and Liangjun Zhang. Autoshape: Real-time shape-aware monocular 3d object detection. In *Proceedings of the IEEE/CVF International Conference on Computer Vision*, pages 15641–15650, 2021.
  - [3] Shaoshuai Shi, Xiaogang Wang, and Hongsheng Li. Pointcnn: 3d object proposal generation and detection from point cloud. In *Proceedings of the IEEE/CVF conference on computer vision and pattern recognition*, pages 770–779, 2019.
  - [4] Alex H Lang, Sourabh Vora, Holger Caesar, Lubing Zhou, Jiong Yang, and Oscar Beijbom. Pointpillars: Fast encoders for object detection from point clouds. In *Proceedings of the IEEE/CVF conference on computer vision and pattern recognition*, pages 12697–12705, 2019.
  - [5] Tianwei Yin, Xingyi Zhou, and Philipp Krahenbuhl. Center-based 3d object detection and tracking. In *Proceedings of the IEEE/CVF conference on computer vision and pattern recognition*, pages 11784–11793, 2021.
  - [6] Danfei Xu, Dragomir Anguelov, and Ashesh Jain. Pointfusion: Deep sensor fusion for 3d bounding box estimation. In *Proceedings of the IEEE conference on computer vision and pattern recognition*, pages 244–253, 2018.
  - [7] Sourabh Vora, Alex H Lang, Bassam Helou, and Oscar Beijbom. Pointpainting: Sequential fusion for 3d object detection. In *Proceedings of the IEEE/CVF conference on computer vision and pattern recognition*, pages 4604–4612, 2020.
  - [8] Chunwei Wang, Chao Ma, Ming Zhu, and Xiaokang Yang. Pointaugmenting: Cross-modal augmentation for 3d object detection. In *Proceedings of the IEEE/CVF Conference on Computer Vision and Pattern Recognition*, pages 11794–11803, 2021.
  - [9] Zhijian Liu, Haotian Tang, Alexander Amini, Xinyu Yang, Huizi Mao, Daniela L Rus, and Song Han. Bevfusion: Multi-task multi-sensor fusion with unified bird’s-eye view representation. In *2023 IEEE international conference on robotics and automation (ICRA)*, pages 2774–2781. IEEE, 2023.
  - [10] Xin Zhao, Zhe Liu, Ruolan Hu, and Kaiqi Huang. 3d object detection using scale invariant and feature reweighting networks. In *Proceedings of the AAAI Conference on Artificial Intelligence*, volume 33, pages 9267–9274, 2019.
  - [11] Hongxiang Cai, Zeyuan Zhang, Zhenyu Zhou, Ziyin Li, Wenbo Ding, and Jihua Zhao. Bevfusion4d: Learning lidar-camera fusion under bird’s-eye-view via cross-modality guidance and temporal aggregation. *arXiv preprint arXiv:2303.17099*, 2023.
  - [12] Tengting Huang, Zhe Liu, Xiwu Chen, and Xiang Bai. Epnet: Enhancing point features with image semantics for 3d object detection. In *Computer Vision–ECCV 2020: 16th European Conference, Glasgow, UK, August 23–28, 2020, Proceedings, Part XV 16*, pages 35–52. Springer, 2020.
  - [13] Andreas Geiger, Philip Lenz, Christoph Stiller, and Raquel Urtasun. Vision meets robotics: The kitti dataset. *The International Journal of Robotics Research*, 32(11):1231–1237, 2013.
  - [14] Jiageng Mao, Minzhe Niu, Chenhan Jiang, Hanxue Liang, Jingheng Chen, Xiaodan Liang, Yamin Li, Chaoqiang Ye, Wei Zhang, Zhenguo Li, et al. One million scenes for autonomous driving: Once dataset. *arXiv preprint arXiv:2106.11037*, 2021.
  - [15] Yinpeng Dong, Caixin Kang, Jinlai Zhang, Zijian Zhu, Yikai Wang, Xiao Yang, Hang Su, Xingxing Wei, and Jun Zhu. Benchmarking robustness of 3d object detection to common corruptions. In *Proceedings of the IEEE/CVF Conference on Computer Vision and Pattern Recognition*, pages 1022–1032, 2023.
  - [16] Kaicheng Yu, Tang Tao, Hongwei Xie, Zhiwei Lin, Tingting Liang, Bing Wang, Peng Chen, Dayang Hao, Yongtao Wang, and Xiaodan Liang. Benchmarking the robustness of lidar-camera fusion for 3d object detection. In *Proceedings of the IEEE/CVF Conference on Computer Vision and Pattern Recognition*, pages 3188–3198, 2023.
  - [17] Zhijian Liu, Haotian Tang, Sibozhu, and Song Han. Semalign: Annotation-free camera-lidar calibration with semantic alignment loss. In *2021 IEEE/RSJ International Conference on Intelligent Robots and Systems (IROS)*, pages 8845–8851. IEEE, 2021.
  - [18] Zhaotong Luo, Guohang Yan, and Yikang Li. Calib-anything: Zero-training lidar-camera extrinsic calibration method using segment anything. *arXiv preprint arXiv:2306.02656*, 2023.
  - [19] Zhe Liu, Tengting Huang, Bingling Li, Xiwu Chen, Xi Wang, and Xiang Bai. Epnet++: Cascade bi-directional fusion for multi-modal 3d object detection. *IEEE transactions on pattern analysis and machine intelligence*, 2022.
  - [20] Ziyang Song, Caiyan Jia, Lei Yang, Haiyue Wei, and Lin Liu. Graphalign++: An accurate feature alignment by graph matching for multi-modal 3d object detection. *IEEE Transactions on Circuits and Systems for Video Technology*, 34(4):2619–2632, 2024.



- [21] Shaoqing Xu, Dingfu Zhou, Jin Fang, Junbo Yin, Zhou Bin, and Liangjun Zhang. Fusionpainting: Multimodal fusion with adaptive attention for 3d object detection. In *2021 IEEE International Intelligent Transportation Systems Conference (ITSC)*, pages 3047–3054. IEEE, 2021.
- [22] Yukang Chen, Yanwei Li, Xiangyu Zhang, Jian Sun, and Jiaya Jia. Focal sparse convolutional networks for 3d object detection. In *Proceedings of the IEEE/CVF Conference on Computer Vision and Pattern Recognition*, pages 5428–5437, 2022.
- [23] Lawrence T Goodnough, Mark E Brecher, Michael H Kanter, and James P AuBuchon. Transfusion medicine—blood transfusion. *New England journal of medicine*, 340(6):438–447, 1999.
- [24] Yingwei Li, Adams Wei Yu, Tianjian Meng, Ben Caine, Jiquan Ngiam, Daiyi Peng, Junyang Shen, Yifeng Lu, Denny Zhou, Quoc V Le, et al. Deepfusion: Lidar-camera deep fusion for multi-modal 3d object detection. In *Proceedings of the IEEE/CVF Conference on Computer Vision and Pattern Recognition*, pages 17182–17191, 2022.
- [25] Xuanyao Chen, Tianyuan Zhang, Yue Wang, Yilun Wang, and Hang Zhao. Futr3d: A unified sensor fusion framework for 3d detection. In *proceedings of the IEEE/CVF conference on computer vision and pattern recognition*, pages 172–181, 2023.
- [26] Yecheol Kim, Konyul Park, Minwook Kim, Dongsuk Kum, and Jun Won Choi. 3d dual-fusion: Dual-domain dual-query camera-lidar fusion for 3d object detection. *arXiv preprint arXiv:2211.13529*, 2022.
- [27] Ziyang Song, Lei Yang, Shaoqing Xu, Lin Liu, Dongyang Xu, Caiyan Jia, Feiyang Jia, and Li Wang. Graphbev: Towards robust bev feature alignment for multi-modal 3d object detection. *arXiv preprint arXiv:2403.11848*, 2024.
- [28] Xiaozhi Chen, Huimin Ma, Ji Wan, Bo Li, and Tian Xia. Multi-view 3d object detection network for autonomous driving. In *Proceedings of the IEEE conference on Computer Vision and Pattern Recognition*, pages 1907–1915, 2017.
- [29] Charles R Qi, Wei Liu, Chenxia Wu, Hao Su, and Leonidas J Guibas. Frustum pointnets for 3d object detection from rgb-d data. In *Proceedings of the IEEE conference on computer vision and pattern recognition*, pages 918–927, 2018.
- [30] Su Pang, Daniel Morris, and Hayder Radha. Clocs: Camera-lidar object candidates fusion for 3d object detection. In *2020 IEEE/RSJ International Conference on Intelligent Robots and Systems (IROS)*, pages 10386–10393. IEEE, 2020.
- [31] Gaurav Pandey, James McBride, Silvio Savarese, and Ryan Eustice. Automatic targetless extrinsic calibration of a 3d lidar and camera by maximizing mutual information. In *Proceedings of the AAAI conference on artificial intelligence*, volume 26, pages 2053–2059, 2012.
- [32] Akio Kodaira, Yiyang Zhou, Pengwei Zang, Wei Zhan, and Masayoshi Tomizuka. Sst-calib: Simultaneous spatial-temporal parameter calibration between lidar and camera. In *2022 IEEE 25th International Conference on Intelligent Transportation Systems (ITSC)*, pages 2896–2902. IEEE, 2022.
- [33] Qilong Zhang and Robert Pless. Extrinsic calibration of a camera and laser range finder (improves camera calibration). In *2004 IEEE/RSJ International Conference on Intelligent Robots and Systems (IROS)(IEEE Cat. No. 04CH37566)*, volume 3, pages 2301–2306. IEEE, 2004.
- [34] Joris Domhof, Julian FP Kooij, and Dariu M Gavrila. An extrinsic calibration tool for radar, camera and lidar. In *2019 International Conference on Robotics and Automation (ICRA)*, pages 8107–8113. IEEE, 2019.
- [35] Yuanfan Xie, Rui Shao, Popo Guli, Bo Li, and Liang Wang. Infrastructure based calibration of a multi-camera and multi-lidar system using apriltags. In *2018 IEEE Intelligent Vehicles Symposium (IV)*, pages 605–610. IEEE, 2018.
- [36] Julius Kümmerle, Tilman Kühner, and Martin Lauer. Automatic calibration of multiple cameras and depth sensors with a spherical target. In *2018 IEEE/RSJ International Conference on Intelligent Robots and Systems (IROS)*, pages 1–8. IEEE, 2018.
- [37] Tao Ma, Zhizheng Liu, Guohang Yan, and Yikang Li. Crlf: Automatic calibration and refinement based on line feature for lidar and camera in road scenes. *arXiv preprint arXiv:2103.04558*, 2021.
- [38] Peyman Moghadam, Michael Bosse, and Robert Zlot. Line-based extrinsic calibration of range and image sensors. In *2013 IEEE International Conference on Robotics and Automation*, pages 3685–3691. IEEE, 2013.
- [39] Jaehyeon Kang and Nakju L Doh. Automatic targetless camera-lidar calibration by aligning edge with gaussian mixture model. *Journal of Field Robotics*, 37(1):158–179, 2020.

- [40] Ioannis Stamos, Lingyun Liu, Chao Chen, George Wolberg, Gene Yu, and Siavash Zokai. Integrating automated range registration with multiview geometry for the photorealistic modeling of large-scale scenes. *International Journal of Computer Vision*, 78:237–260, 2008.
- [41] Zixuan Bai, Guang Jiang, and Ailing Xu. Lidar-camera calibration using line correspondences. *Sensors*, 20(21):6319, 2020.
- [42] Haileleol Tibebu, Jamie Roche, Varuna De Silva, and Ahmet Kondo. Lidar-based glass detection for improved occupancy grid mapping. *Sensors*, 21(7):2263, 2021.
- [43] Nick Schneider, Florian Piewak, Christoph Stiller, and Uwe Franke. Regnet: Multimodal sensor registration using deep neural networks. In *2017 IEEE intelligent vehicles symposium (IV)*, pages 1803–1810. IEEE, 2017.
- [44] Ganesh Iyer, R Karnik Ram, J Krishna Murthy, and K Madhava Krishna. Calibnet: Geometrically supervised extrinsic calibration using 3d spatial transformer networks. In *2018 IEEE/RSJ International Conference on Intelligent Robots and Systems (IROS)*, pages 1110–1117. IEEE, 2018.
- [45] Kaiwen Yuan, Zhenyu Guo, and Z Jane Wang. Rggnet: Tolerance aware lidar-camera online calibration with geometric deep learning and generative model. *IEEE Robotics and Automation Letters*, 5(4):6956–6963, 2020.
- [46] Zachary Taylor and Juan Nieto. Motion-based calibration of multimodal sensor extrinsics and timing offset estimation. *IEEE Transactions on Robotics*, 32(5):1215–1229, 2016.
- [47] Chanoh Park, Peyman Moghadam, Soohwan Kim, Sridha Sridharan, and Clinton Fookes. Spatiotemporal camera-lidar calibration: A targetless and structureless approach. *IEEE Robotics and Automation Letters*, 5(2):1556–1563, 2020.
- [48] Xudong Lv, Boya Wang, Ziwen Dou, Dong Ye, and Shuo Wang. Lccnet: Lidar and camera self-calibration using cost volume network. In *Proceedings of the IEEE/CVF Conference on Computer Vision and Pattern Recognition*, pages 2894–2901, 2021.
- [49] Juraj Peršić, Luka Petrović, Ivan Marković, and Ivan Petrović. Spatiotemporal multisensor calibration via gaussian processes moving target tracking. *Ieee transactions on robotics*, 37(5):1401–1415, 2021.
- [50] Alexander Tsaregorodtsev, Johannes Muller, Jan Strohbeck, Martin Herrmann, Michael Buchholz, and Vasileios Belagiannis. Extrinsic camera calibration with semantic segmentation. In *2022 IEEE 25th International Conference on Intelligent Transportation Systems (ITSC)*, pages 3781–3787. IEEE, 2022.
- [51] Pawel Rotter, Maciej Klemiato, and Pawel Skruch. Automatic calibration of a lidar-camera system based on instance segmentation. *Remote Sensing*, 14(11):2531, 2022.
- [52] Alexander Kirillov, Eric Mintun, Nikhila Ravi, Hanzi Mao, Chloe Rolland, Laura Gustafson, Tete Xiao, Spencer Whitehead, Alexander C Berg, Wan-Yen Lo, et al. Segment anything. In *Proceedings of the IEEE/CVF International Conference on Computer Vision*, pages 4015–4026, 2023.
- [53] Yuxuan Xiao, Yao Li, Chengzhen Meng, Xingchen Li, and Yanyong Zhang. Calibformer: A transformer-based automatic lidar-camera calibration network. *arXiv preprint arXiv:2311.15241*, 2023.
- [54] Yuenan Hou, Xinge Zhu, Yuexin Ma, Chen Change Loy, and Yikang Li. Point-to-voxel knowledge distillation for lidar semantic segmentation. In *IEEE Conference on Computer Vision and Pattern Recognition*, pages 8479–8488, 2022.
- [55] Xinge Zhu, Hui Zhou, Tai Wang, Fangzhou Hong, Yuexin Ma, Wei Li, Hongsheng Li, and Dahua Lin. Cylindrical and asymmetrical 3d convolution networks for lidar segmentation. In *IEEE Conference on Computer Vision and Pattern Recognition*, pages 9939–9948, 2021.
- [56] Xinge Zhu, Hui Zhou, Tai Wang, Fangzhou Hong, Wei Li, Yuexin Ma, Hongsheng Li, Ruigang Yang, and Dahua Lin. Cylindrical and asymmetrical 3d convolution networks for lidar-based perception. *IEEE Transactions on Pattern Analysis and Machine Intelligence*, 2021.
- [57] Liang-Chieh Chen, George Papandreou, Florian Schroff, and Hartwig Adam. Rethinking atrous convolution for semantic image segmentation. *arXiv preprint arXiv:1706.05587*, 2017.